Structure of the trigonal crystal form of bovine annexin IV

Giuseppe ZANOTTI*[1], Giorgio MALPELI†, Francesca GLIUBICH*‡, Claudia FOLLI†, Monica STOPPINI§, Luca OLIVI‖, Adolfo SAVOIA‖ and Rodolfo BERNI†

*Department of Organic Chemistry, University of Padova, and Biopolymer Research Center, C.N.R., 35131 Padova, Italy, †Institute of Biochemical Sciences, University of Parma, 43100 Parma, Italy, ‡Institute of Pharmaceutical Chemistry, University of Milan, 20135 Milan, Italy, §Department of Biochemistry, University of Pavia, 27100 Pavia, Italy, and ‖Sincrotrone Trieste, Basovizza, 34012 Trieste, Italy

The structure of a trigonal crystal form of N-terminally truncated [des-(1–9)] bovine annexin IV, an annexin variant that exhibits the distinctive property of binding both phospholipids and carbohydrates in a Ca^{2+}-dependent manner, has been determined at 3 Å (0.3 nm) resolution [space group: R3; cell parameters: $\mathbf{a} = \mathbf{b} = 118.560$ (8) Å and $\mathbf{c} = 82.233$ (6) Å]. The overall structure of annexin IV, crystallized in the absence of Ca^{2+} ions, is highly homologous to that of the other known members of the annexin family. The trimeric assembly in the trigonal crystals of annexin IV is quite similar to that found previously in non-isomorphous crystals of human, chicken and rat annexin V and to the subunit arrangement in half of the hexamer of hydra annexin XII. Moreover, it resembles that found in two-dimensional crystals of human annexin V bound to phospholipid monolayers. The propensity of several annexins to generate similar trimeric arrays supports the hypothesis that trimeric complexes of such annexins, including annexin IV, may represent the functional units that interact with membranes.

INTRODUCTION

Annexin is the general name of a family of proteins characterized by a highly conserved fold, consisting of four domains (eight in annexin VI). These domains, similar to one another in both primary and secondary structures, consist of the assembly of five α-helices. The four domains are arranged in a highly symmetrical slightly flattened array, with opposing concave and convex faces [1]. The physiological role of the numerous members of the family so far identified is still unclear: proposed functions include inhibition of coagulation, regulation of phospholipase A_2 activity, Ca^{2+}-ion-channel activity, initiation of membrane fusion in exocytosis and endocytosis and interaction with cytoskeletal elements [2–4]. Functional properties exhibited by annexins appear to be related to the feature, common to all members of the family, of binding Ca^{2+} ions. In turn, this interaction promotes the binding of the protein to phospholipid-containing membranes and the aggregation of phospholipid vesicles. The binding to a phospholipid bilayer is associated, at least for some of the members of the family, with the formation of voltage-gated Ca^{2+} ion channels [5]. Ion-channel activity has been suggested for a hydrophilic central pore of monomeric annexin V [6] and subsequently confirmed by site-directed mutagenesis studies [7]. Electron-microscopic analysis of negatively stained two-dimensional crystals bound to phospholipid monolayers has indicated that trimers of annexin V bind peripherally to the membrane, with their convex side harbouring the Ca^{2+}-binding sites [7,8]. Based on the structure of hydra annexin XII, Luecke et al. [9] have suggested a different mode of both annexin binding to membranes and ion conduction. According to the latter authors, annexin monomers associate to form a hexamer that spans the membrane bilayer, and the channel across the membrane is represented by the central pore of the macromolecular assembly.

The amino acid sequences of the various members of the annexin family are well conserved, except for their N-termini, which are quite variable. This variability has been attributed to specific functions of the N-termini: for example, the annexin II N-terminal region binds protein p11 with high affinity, and this interaction is inhibited by protein kinase C phosphorylation of a serine residue lying within the sequence mediating p11 binding [10]; by contrast, phosphorylation of the N-terminus of annexin I appears to play a regulatory role in phospholipid vesicle aggregation [11].

Besides exhibiting Ca^{2+}-dependent phospholipid binding similar to that of the other members of the annexin family [12,13], bovine annexin IV has been shown to interact with carbohydrates in a Ca^{2+}-dependent manner [13,14]. The amino acid sequence of bovine annexin IV, which has been deduced from the cDNA sequence, consists of 318 residues [13,15]. When SDS/PAGE was carried out in the absence of reducing agents, two bands, corresponding to apparent masses of 33 and 41 kDa, were found in the electrophoretic pattern of annexin IV, either purified from bovine kidney or obtained as a recombinant protein [13]. It has been shown by MS and site-directed mutagenesis that the higher-molecular-mass component is formed on protein dimerization in non-reducing conditions: two monomers are connected by a disulphide bridge between two Cys-198 residues, to generate a dimer with an apparent molecular mass of 41 kDa [13]. However, the mechanism leading to dimer formation is not yet known.

The crystal structures of several annexins have been determined so far: annexin I [16], II [17], III [18], V [1,19–21], VI [22,23], XII [9]. The structure of a monoclinic crystal form of bovine annexin IV, complexed with Ca^{2+} ions, has also been obtained by R. B. Sutton and S. R. Sprang (Southwest Medical Center, University of Texas, Dallas, TX, U.S.A.) and the atomic co-ordinates have been deposited as 1ANN at the Brookhaven Protein Data Bank [24]. We describe here the structure at 3 Å (0.3 nm) resolution of a trigonal crystal form of Ca^{2+}-free N-terminally truncated annexin IV purified from bovine kidney.

EXPERIMENTAL

Protein purification and crystallization

Pure annexin IV was obtained from bovine kidney as follows. Since in previous purification experiments bovine annexin IV was found to co-purify with 3-hydroxyanthranilate dioxygenase (3-HAO, EC 1.13.11.6), by using the chromatographic steps

Abbreviations used: 3-HAO, 3-hydroxyanthranilate dioxygenase; r.m.s., root mean square.

[1] To whom correspondence should be addressed.

Table 1 Summary of data collection and refinement

Some 45048 measurements were merged into 8114 independent reflections with intensity greater than 0. R_{merge}, defined as $\Sigma(I - \langle I \rangle)/\Sigma I$, was 0.049. Standard values for bond lengths and angles were taken from file param19x.pro, distributed with the package X-PLOR [27].

Completeness of the data set	Resolution interval (Å)	Percentage
	$5.98 < d < 55.0$	86
	$3.50 < d < 5.98$	98
	$2.99 < d < 3.50$	87
	$2.99 < d < 55.0$	93
R-factor (6717 reflections in the resolution range 7–2.99 Å)	0.190	
R_{free} (800 reflections)	0.269	
Total number of non-hydrogen protein atoms	3039	
r.m.s. deviation from bonds standard values (Å)	0.019	
r.m.s. deviation from angles standard values (°)	3.57	

reported here, determination of 3-HAO activity allowed us to follow, at the same time, the purification of the annexin. Briefly, bovine kidney was homogenized in buffer A [0.1 M potassium phosphate, 20% (v/v) glycerol, 3 mM 2-mercaptoethanol, pH 7.4]; the homogenate was centrifuged and the pellet discarded. The protein fraction resulting from the precipitation of the supernatant in the 34–62%-satd. $(NH_4)_2SO_4$ was resuspended in buffer B [5 mM potassium phosphate, 20% (v/v) glycerol, 3 mM 2-mercaptoethanol, pH 7.4] and dialysed exhaustively against the same buffer containing the protease inhibitor PMSF (0.1 mM). The preparation was then applied to a DEAE-Sephadex A-50 column (Pharmacia, Uppsala, Sweden), equilibrated with buffer B and developed with a linear gradient from buffer B to buffer A. The fractions containing 3-HAO activity, which was determined as described by Malherbe et al. [25], were obtained at the end of the gradient and were pooled and concentrated by precipitation with 80%-satd. $(NH_4)_2SO_4$. The protein preparation was then dialysed against 10 mM Tris/HCl, pH 7.4, containing 20% (v/v) glycerol and 0.02% (v/v) 2-mercaptoethanol, and applied to a Blue-Sepharose CL-4B column (Pharmacia) equilibrated and eluted with the same buffer. 3-HAO activity was recovered in the flow-through fractions, which were pooled and concentrated by ultrafiltration through a YM-10 membrane in an Amicon cell (Amicon, Beverly, MA, U.S.A.). The concentrated solution was chromatographed on an Ultrogel AcA 54 (Biosepra, Locke Drive, MA, U.S.A.) column, equilibrated and developed with buffer A. Analysis by SDS/PAGE of the fractions containing 3-HAO activity revealed a single band corresponding to a molecular mass of approx. 33 kDa. However, non-denaturing PAGE resolved two components, which could be purified by FPLC on a Protein Pak Glass DEAE-4 PW column (Waters Associate Inc., Milford, MA, U.S.A.), equilibrated with 20 mM Tris/HCl/1 mM dithiothreitol, pH 7.4, and developed with a linear NaCl gradient (0–0.1 M). One of the two components was 3-HAO. The other could be identified unambiguously as N-terminally truncated annexin IV on the basis of sequence analysis of its N-terminus by the use of a HPG 1000A protein sequenator (Hewlett–Packard), with routine 3.0 chemistry method and PTH-4M HPLC method (H.P. Technical Note 95-1). By comparison with the known sequence of bovine annexin IV as deduced from the cDNA sequence [13,15], our annexin preparation lacks the first nine amino acid residues, whereas residues 10–30 were found to be identical with those deduced from the cDNA.

Single crystals of N-terminally truncated bovine annexin IV grew at room temperature (295 K) in sitting-drop vapour-diffusion experiments. Droplets (3 μl) containing protein at a concentration of approx. 10 mg/ml in the presence of 1 M $(NH_4)_2SO_4$/50 mM Tris/HCl, pH 7.3, were equilibrated with a reservoir solution (0.5 ml) containing 1.4 M $(NH_4)_2SO_4$, 10 mM 2-mercaptoethanol and 0.1 M sodium citrate, pH 5.0. Bipyramidal crystals of approximate size $0.2 \times 0.2 \times 0.1$ mm^3 could be obtained in 1–2 weeks.

Data collection and processing

Since the crystals of annexin IV were found to be very unstable when exposed at room temperature to a conventional X-ray source, data were collected at 100 K at the diffraction beam line of the synchrotron ELETTRA (Trieste, Italy). The ring was operated at 1.997 GeV with a mean current of 140 mA. One crystal was used for the collection of an entire data set at 3 Å resolution, using a wavelength of 1.30 Å. The crystal was transferred from its mother liquor to a cryo-protectant solution obtained by mixing the precipitant solution [1.4 M $(NH_4)_2SO_4$, 10 mM 2-mercaptoethanol, 0.1 M sodium citrate, pH 5.0] with glycerol in a 2:1 (v/v) ratio. After a few minutes, the crystal was picked up with a loop and immediately frozen by flushing liquid nitrogen. After collecting 83 frames of 2° rotation each, the crystal was reoriented in a random way and another 67 frames with the same angular rotation were measured. The spectrum was recorded on an image-plate detector of 180 mm diameter (MAR Research), with a crystal-to-detector distance of 170 mm. Data were processed with the software XDS [26] and were consistent with an R3 space group: cell parameters are $\mathbf{a} = \mathbf{b} =$ 118.560 (8) Å, $\mathbf{c} = 82.233$ (6) Å (hexagonal indexing). Assuming the presence of one molecule per asymmetric unit and a molecular mass of 33 kDa, V_M is 3.37 Å^3/Da and the solvent content about 63% of the total crystal volume.

Structure solution and refinement

The structure was solved by the molecular replacement method, using as a search model the structure of the monoclinic crystal form of bovine annexin IV deposited by Sutton and Sprang at the Brookhaven Protein Data Bank (1ANN) [24]. The model, deprived of amino acids 4–9 and of Ca^{2+} ions and solvent molecules, was inserted into a cell of 100 Å sides, and its Patterson map was rotated and correlated with the rhombohedral Patterson map, calculated with data from 8 to 3 Å resolution. The highest maximum of the correlation function was 21.5 with a root mean square (r.m.s.) deviation from mean intensity of 2.6, the second and the third maxima being 18.0 and 12.6. The translation function, carried on with the highest four solutions of the rotation, resulted in the equivalence for the first two solutions, with a correlation coefficient of 40 and a crystallographic *R* factor of 0.39.

A rigid body refinement on the rotated and translated model reduced the *R* factor on all reflections, up to 3 Å resolution, to 0.43. A subsequent molecular-dynamics step, using a slow-cooling protocol [27] from 500 to 300 K, followed by thermal parameter refinement, reduced the *R* factor to 0.26. From this point on, 15 cycles of minimization, alternated with visual inspection of maps and manual adjustments of the model, reduced the *R* factor to the final value of 0.190 for 6717 reflections in the resolution range from 7 to 2.99 Å and the R_{free} factor to 0.269 for the remaining 801 reflections. Owing to the relatively low resolution, solvent molecules were not introduced in the

model. A summary of data-collection statistics, along with the statistics for the final model, are reported in Table 1. Atomic co-ordinates have been deposited as 1AOW at the Brookhaven Protein Data Bank for immediate release.

Rotation and translation functions were calculated using the software AMORE [28] contained in the CCP4 package [29]; the refinement was performed with the program X-PLOR [27] and maps and model were visualized on a Silicon Graphics IRIS 4D workstation using the program TOM [30].

RESULTS AND DISCUSSION

Quality of the model

A Ramachandran plot [31] of the annexin IV model shows that 80 and 17% of the residues lie in the most favoured and additionally allowed regions respectively, seven residues lie in the generously allowed regions and one, Lys-99, lies in a disallowed region, as defined by program PROCHECK [32]. The other tests of the same program suggest that additional indicators of structure quality are consistent with, and sometimes better than, a 3 Å resolution structure.

The overall *B* factor is 20.6 and 20.4 Å^2 for main-chain and side-chain atoms respectively. A plot of mean thermal parameters as a function of the residue number is reported in Figure 1. Two strongly disordered regions, encompassing residues 99–102 and 186–190, are clearly present: in these two areas the electron density is quite poor and, particularly for residues 99–102, the model has been built tentatively. Other relatively flexible areas comprise amino acids 164–168, 215–218 and 257–262, all corresponding to loop regions. Finally, the electron density for some residues (269–272) of helix IVB is not clearly defined, a fact that could perhaps be attributed to the limited resolution of the data rather than to actual disorder in the structure.

Overall structure of des-(1–9)-annexin IV and comparison with other annexins

A schematic model of bovine annexin IV, showing the elements of secondary structure, is given in Figure 2 (top). It should be noticed that the protein we have crystallized lacks residues 1–9 (see the Experimental section). Therefore our model starts from residue 10 and ends with residue 318. The sequence numbering, with the indication of the corresponding secondary-structure elements, is presented in the bottom panel of Figure 2. The overall structure is very similar to that of the other annexins of known tertiary structure and consists of four similar domains, each containing five α-helical segments. The assignment of secondary-structure elements is necessarily preliminary in our model, owing to the relatively limited resolution, but a comparison with other known annexins (see below) shows a nearly perfect agreement with regard to the positions of the α-helices in the four domains present in the tertiary structure.

A superposition of the α-carbon atoms of our model with those of the monoclinic crystal form of bovine annexin IV (R. B. Sutton and S. R. Sprang) gives an overall r.m.s. deviation of 0.98 Å, but differences larger than 2 Å can be observed in five specific regions: at the N-terminal region (residues 10–11), and at regions from 98 to 102, from 156 to 163, from 186 to 195 and from 258 to 261. The lack of the first nine amino acids at the N-terminus justifies significant r.m.s. deviations in that area. The loop around residue 100 (loop 99–103), which is one of the potential Ca^{2+}-binding sites, in accordance with features previously established for other annexins [2], does not bind any Ca^{2+} ion in both the monoclinic and trigonal crystal forms of bovine annexin IV. In addition, the above loop is totally disordered in both annexin IV structures, such that possible differences cannot be considered significant. The area encompassing residues 156–163 is the relatively long strand that connects domain II and III and appears to be quite mobile. The area corresponding to residues 186–195, which includes helix IIIB, is partially involved in intermolecular contacts (see below). The area corresponding to residues 258–261 is a loop that binds Ca^{2+} in the annexin IV monoclinic crystal model. By comparison with our model of Ca^{2+}-free annexin IV, the interactions of Ca^{2+} ions with loops 27–30 in domain I and 258–261 in domain IV of the monoclinic crystal form of annexin IV do not appear to induce dramatic protein conformational changes.

A comparison of the present structure with those of annexins V [19] and III [18] is illustrated in Figure 3. The overall r.m.s. differences between equivalent α-carbon atoms are 2.15 and 1.78 Å respectively. Despite these relatively large values, the

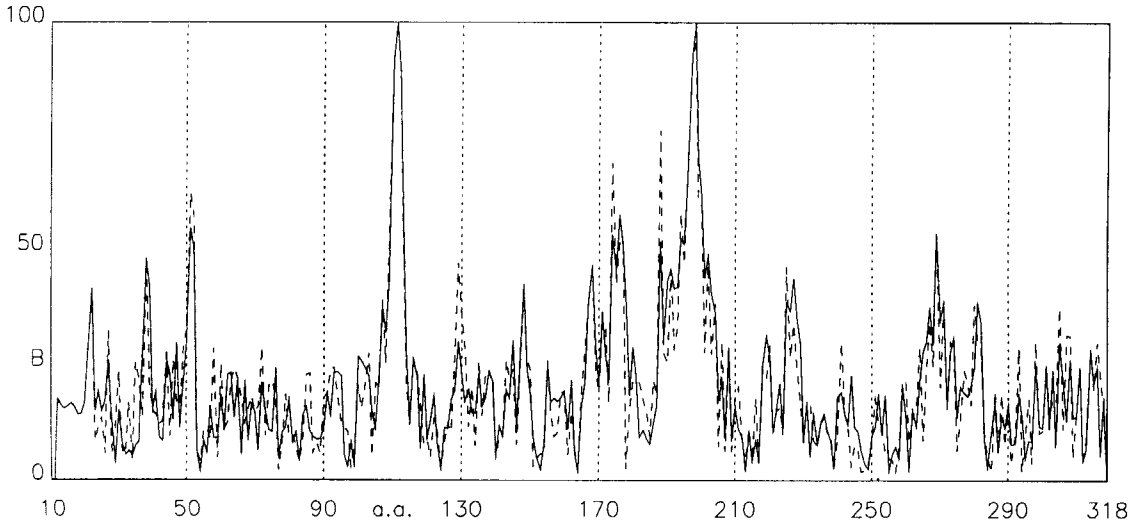

Figure 1 Mean *B* value as a function of the number of the residue (a.a.) for main-chain atoms (——) and side-chain atoms (– – – –)

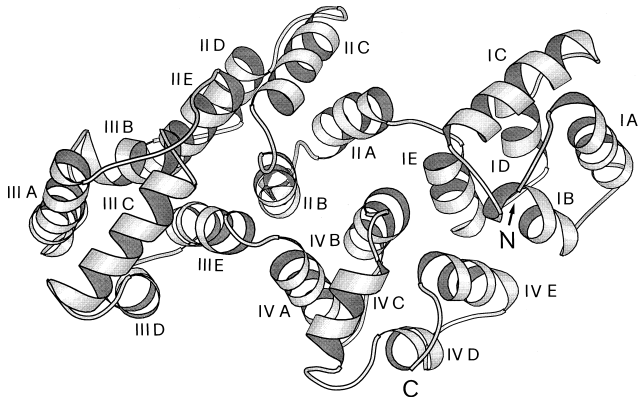


```
        10                  30                  50
         A SGFNAAEDAQ TLRKAMKGLG TDEDAIINVL AYRSTAQRQE IRTAYKTTIG
               ----I A------        ----I B---  -----I C-------

        70                  90                  110
RDLMDDLKSE LSGNFEQVIL GMMTPTVLYD VQEVRKAMKG AGTDEGCLIE ILASRTPEEI
  --I D---    ----I E----  ----II A-----     ----II B----    ----

       130                 150                 170
RRINQTYQLQ YGRSLEDDIR SDTSFMFQRV LVSLSAGGRD ESNYLDDALM RQDAQDLYEA
II C-----      ---II D--  ----II E-----           -------III A---

       190                 210                 230
GEKKWGTDEV KFLTVLCSRN RNHLLHVFDE YKRIAQKDIE QSIKSETSGS FEDALLAIVK
--       ---III B--   -----III C-----    --III D--  ----III E----

       250                 270                 290
CMRNKSAYFA ERLYKSMKGL GTDDDTLIRV MVSRAEIDML DIRANFKRLY GKSLYSFIKG
--  ---IV A-------       ----IV B----    ---IV C---       --IV D-

       310
DTSGDYRKVL LILCGGDD
   ----IV E----
```

Figure 2 (Top) Schematic drawing of the model of the trigonal crystal form of bovine annexin IV, prepared with program MOLSCRIPT [33] and (bottom) positions of secondary-structure elements

In the drawing the roman numbers from I to IV refer to the four domains and the letters from A to E refer to the five α-helices present in each domain. The amino acid sequence of bovine annexin IV [13,15] starts with residue 10, which is the first present in our preparation of annexin IV. Secondary-structure elements were assigned according to the program PROCHECK [32]. α-Helical regions are underlined.

Figure 3 Superposition of the Cα chain trace of annexin IV (this paper, thick line) with annexin V [19] (co-ordinates 1ALA from Brookhaven Protein Data Bank) (top) and annexin III [18] (co-ordinates 1AXN from Brookhaven Protein Data Bank) (bottom)

overall conformation is highly preserved: single domains of two models can be superimposed separately with a much lower r.m.s. deviation, a further indication of the existence of differences in the relative orientation of the domains owing to the different geometry of the elements connecting the domains. Definite differences in conformations are observed only in limited areas. The C-terminal portion of helix D in domain III (residues 224–228) and the strand connecting domains II and III (residues 158–166) have different conformations in our structure as compared with annexin V. The latter area also differs from that of annexin III, along with the loop from residue 183 to 187, which connects helices A and B in domain III. The loop 99–103, which is quite disordered in bovine annexin IV as mentioned above, is on the contrary well ordered in other members of the family.

As reported above, it has been found that bovine annexin IV gives two 33 and 41 kDa bands on SDS/PAGE under non-reducing conditions, and only one 33 kDa band on SDS/PAGE under reducing conditions [13]. In addition, it has been shown that the 41 kDa band corresponds to a dimeric form of annexin IV, which is generated by the cross-linking of two 33 kDa monomers via a disulphide bond between their Cys-198 residues [13]. On the basis of our three-dimensional structure of bovine annexin IV, we can conclude that a dramatic conformational change must take place to allow the exposure of Cys-198 on the protein surface, thus permitting the formation of a disulphide bond cross-linking two annexin monomers. It is tempting to speculate that, on exposure to SDS, annexin IV may initially undergo the above change, such that a significant part of the protein molecules could form intermolecular disulphide bonds between residues of Cys-198, under non-reducing conditions. This mechanism for dimer formation is consistent with our observations that bovine annexin IV is eluted during gel-filtration chromatography (Ultrogel AcA54), carried out in non-denaturing conditions, as a monomer with molecular mass of approx. 33 kDa and that such a protein can generate the 33 and 41 kDa bands on SDS/PAGE under non-reducing conditions and only the 33 kDa band on SDS/PAGE under reducing conditions (R. Berni, G. Malpeli and C. Folli, unpublished work). Thus the presence of denaturing conditions appears to be a requirement for dimer formation.

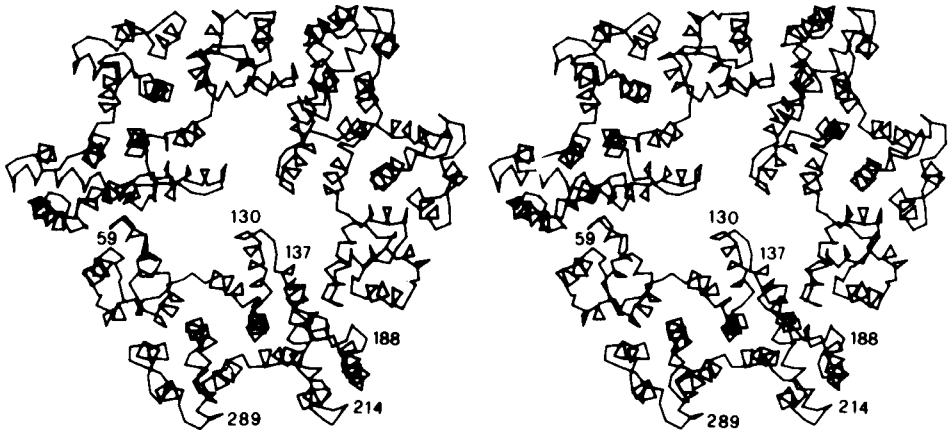

Figure 4 Stereo view of the trimeric arrangement around the crystallographic threefold axis in the trigonal crystals of annexin IV

The view is along the symmetry axis. The figure can be compared with Figure 12(a) of ref. [8], where the crystal structure of annexin V is shown in the same orientation.

Interaction of annexins with membranes

Several hypotheses have been put forward with regard to the interaction of annexins with membranes and the formation of Ca^{2+} ion channels. A three-dimensional reconstruction from electron micrographs of two-dimensional crystals of annexin V bound to phospholipid monolayers could be clearly interpreted in terms of complexes of three annexin molecules bound, with their convex sides, to the membrane surface [8]. The density was shown to correspond, after minor adjustments of the relative orientations of modules (I/IV) and (II/III), to the trimeric assembly found in the trigonal crystal form of human annexin V [19]. It has been suggested that the above change occurring in the membrane-bound annexin relative to the X-ray structure is induced by membrane binding [8]. In particular, the presence of the positive charges of Ca^{2+} ions would allow the interaction of annexin V with the negatively charged phospholipid headgroups of a planar monolayer and promote the relative reorientation of the domains in such a way that they become co-planar to the membrane. As a result, the membrane-bound annexin molecules would lose their curved shape and become flat [8]. Consistent with the formation of trimeric complexes of annexin V in both two-dimensional and three-dimensional crystals, studies carried out in solution have indicated that annexin V forms Ca^{2+}-dependent trimeric units on phospholipid vesicles [34].

It is worth noting that the trimeric mode of assembly established for the trigonal crystals of human annexin V [19] is also present in the isomorphous trigonal crystals of chicken annexin V [20] and in the non-isomorphous trigonal crystals of rat annexin V [21]. In addition, in the hexameric structure of hydra annexin XII [9], two trimers, each similar to the trimers found in the trigonal crystals of annexin V, are stacked one on the top of the other, related by a twofold axis, and the contact between them is represented by the surface that should bind to the phospholipid membranes according to the model of Voges et al. [8]. A complete insertion into phospholipid bilayers, at variance with the superficial binding suggested by Voges et al. [8] and Liemann et al. [7] for annexin V, has been proposed for the hexamer of hydra annexin XII [9].

The way the three annexin IV molecules are arranged around the threefold axis in our trigonal crystals (Figure 4) is virtually identical with that found in the non-isomorphous trigonal crystals of human [19], chicken [20] and rat [21] annexin V (compare, for example, the trimer for annexin IV crystals shown in Figure 4 with that for human annexin V crystals presented in Figure 12 of ref. [8]). Moreover, the intermolecular contacts in the trimer for annexin IV crystals are also similar to those present in hexameric hydra annexin XII [9]. In particular, the three annexin IV molecules related by the threefold axis present extensive intermolecular contacts: residues of helices IA and IC and of the loop connecting the latter to helix ID are at a short distance from residues of helices IID, IIE and IIIB of a symmetry-related molecule. Several hydrogen bonds and polar interactions, the location of which is summarized in Table 2, appear to stabilize the formation of the trimer in the crystal. Most of the residues present in the intermolecular contact areas are conserved in the other annexin molecules that form trimeric complexes in three-dimensional crystals, and approximately the same kinds of

Table 2 Hydrogen bonds and polar interactions formed between the reference molecule and a molecule related by the equivalent position $(-y, x-y, z)$

The listed contacts repeat three times in a trimer. Only the interactions for which distances between two polar atoms are shorter than 3.6 Å are listed. The interactions are considered hydrogen bonds when the distance between the potential H donor and acceptor atoms is $\leqslant$ 3.2 Å.

Atom 1	Atom 2	Distance (Å)
Arg-23 NH2	Glu-189 $O\epsilon_1$; $O\epsilon_2$	3.2; 2.8
Lys-56 Nζ	Arg-140 NH_2	3.0
Thr-57 Oγ1	Gly-158 N	3.1
Thr-57 O	Ser-198 Oγ	3.2
Thr-58 O	Thr-194 $O\gamma_1$	2.4
Arg-61 NH_1	Arg-149 NH_1	2.7
Asp-62 N	Arg-140 NH_2	3.2
Asp-62 $O\delta_1$	Glu-136 $O\epsilon_1$; $O\epsilon_2$	2.8; 3.1
Lys-56 Nζ	Glu-136 $O\epsilon_1$	3.5
Thr-57 $O\gamma_1$	Ser-153 O	3.4
Thr-57 O	Ser-153 Oγ	3.5
Thr-57 O	Thr-194 $O\gamma_1$	3.4
Thr-58 O	Val-190 O	3.5
Ile-59 O	Arg-149 Nϵ	3.4

interactions between monomers are possible, at least in principle. In conclusion, our data further indicate the propensity of several members of the annexin family, including annexin IV, to self-associate to generate non-covalent trimers. Annexin trimers might be of physiological significance as they might represent the functional units binding to membranes.

The technical assistance of Alessandra Cobianchi is gratefully acknowledged. We thank R. Pavan and M. Tognolin for help with preparation of the drawings. C.F. is a recipient of a fellowship from AIRC, Milan, Italy. This work was supported by CNR and by MURST, Rome, Italy.

REFERENCES

1 Huber, R., Römisch, J. and Paques, E. P. (1990) EMBO J. **9**, 3867–3874
2 Swairjo, M. A. and Seaton, B. A. (1994) Annu. Rev. Biophys. Biomol. Struct. **23**, 193–213
3 Raynal, P. and Pollard, H. B. (1994) Biochim. Biophys. Acta **1197**, 63–93
4 Liemann, S. and Lewitt-Bentley, A. (1995) Structure **3**, 233–237
5 Rojas, E., Pollard, H. B., Haigler, H. T., Parra, C. and Burns, A. L. (1990) J. Biol. Chem. **265**, 21207–21215
6 Demange, P., Voges, D., Benz, J., Liemann, S., Göttig, P., Berendes, R., Burger, A. and Huber, R. (1994) Trends Biochem. Sci. **19**, 272–276
7 Liemann, S., Benz, J., Burger, A., Voges, D., Hofmann, A., Huber, R. and Göttig, P. (1996) J. Mol. Biol. **258**, 555–561
8 Voges, D., Derendes, R., Burger, A., Demange, P., Baumeister, W. and Huber, R. (1994) J. Mol Biol. **238**, 199–213
9 Luecke, H., Chang, B. T., Maillard, W. S., Schlaepfer, D. D. and Haigler, H. T. (1995) Nature (London) **378**, 512–515
10 Jost, M. and Gerke, V. (1996) Biochim. Biophys. Acta **1313**, 283–289
11 Porte, F., de Santa Barbara, P., Phalipou, S., Liautard, J. P. and Widada, J. S. (1996) Biochim. Biophys. Acta **1293**, 177–184
12 Junker, M. and Creutz, C. E. (1994) Biochemistry **33**, 8930–8940
13 Kojima, K., Yamamoto, K., Irimura, T., Osawa, T., Ogawa, H. and Matsumoto, I. (1996) J. Biol. Chem. **271**, 7679–7685

Received 9 June 1997/8 August 1997; accepted 10 September 1997

14 Kojima, K., Ogawa, H., Seno, N. and Matsumoto, I. (1992) J. Chromatogr. **599**, 323–330
15 Hamman, H. C., Gaffey, L. C., Lynch, K. R. and Creutz, C. E. (1988) Biochem. Biophys. Res. Commun. **156**, 660–667
16 Weng, X., Luecke, H., Song, I. S., Kang, D. S., Kim, S.-H. and Huber, R. (1993) Protein Sci. **2**, 448–458
17 Burger, A., Berendes, R., Liemann, S., Benz, J., Hofmann, A., Göttig, P., Huber, R., Gerke, V., Thiel, C., Römisch, J. and Weber, K. (1996) J. Mol. Biol. **257**, 839–847
18 Favier-Perron, B., Lewitt-Bentley, A. and Russo-Marie, F. (1996) Biochemistry **35**, 1740–1744
19 Huber, R., Berendes, R., Burger, A., Schneider, M., Karshikov, A. and Luecke, H. (1992) J. Mol. Biol. **260**, 638–643
20 Bewley, M. C., Boustead, C. M., Walker, J. M. and Waller, D. A. (1993) Biochemistry **32**, 3923–3929
21 Concha, N. O., Head, J. F., Kaetzel, M. A., Dedman, J. R. and Seaton, B. A. (1993) Science **261**, 1321–1324
22 Benz, J., Bergner, A., Hofmann, A., Demange, P., Göttig, Liemann, S., Huber, R. and Voges, D. (1996) J. Mol. Biol. **260**, 638–643
23 Kawasaki, H., Avilasakar, A., Creutz, C. E. and Kretzinger, R. H. (1996) Biochim. Biophys. Acta **1313**, 277–282
24 Bernstein, F. C., Koetzle, T. F., Williams, G. J. B., Meyers, E. F., Brice, M. D., Rodgers, J. R., Kennard, O., Shimanouchi, T. and Tasumi, M. (1997) J. Mol. Biol. **112**, 572–574
25 Malherbe, P., Kohler, C., Da Prada, M., Lang, G., Kiefer, V., Schwarcz, R., Lahm, H.-W. and Cesura, A. M. (1994) J. Biol. Chem. **269**, 13792–13797
26 Kabsch, W. (1988) J. Appl. Crystallogr. **21**, 916–924
27 Brünger, A. T., Kuriyan, K. and Karplus, M. (1987) Science **235**, 458–460
28 Navaza, J. (1994) Acta Crystallogr. **A50**, 157–163
29 Collaborative Computational Project, Number 4 (1994) Acta Crystallogr. **D50**, 760–763
30 Jones, T. A. (1978) J. Appl. Crystallogr. **11**, 268–272
31 Ramachandran, G. N., Ramakrishnan, C. and Sasisekharan, V. (1963) J. Mol. Biol. **7**, 95–99
32 Laskowski, R. A., MacArthur, M. W., Moss, D. S. and Thornton, J. M. (1993) J. Appl. Crystallogr. **26**, 283–291
33 Kraulis, P. J. (1991) J. Appl. Crystallogr. **24**, 946–950
34 Concha, N. O., Head, J. F., Kaetzel, M. A., Dedman, J. R. and Seaton, B. A. (1992) FEBS Lett. **314**, 159–162